© 2017 IJSRST | Volume 3 | Issue 3 | Print ISSN: 2395-6011 | Online ISSN: 2395-602X
Themed Section: Science and Technology

High Performance Asymmetric Supercapacitor based on spinel Co_3O_4 nanoparticles

Selvapriya R*[1], Alagar M[1]
Centre for Research and Post Graduate Department of Physics, Ayya Nadar Janaki Ammal College, Sivakasi,Tamil Nadu, India

ABSTRACT

We report a facile synthesis and characterization of spinel Co_3O_4 nanostructures on its utilization as electrode material for asymmetric supercapacitors by co-precipitation method. The as-synthesized nanostructure was characterized by X-ray diffraction(XRD),Fourier transform infrared spectroscopy(FTIR) and Scanning electron microscopy(SEM). Electrochemical behaviour of the Co_3O_4 electrode performance was characterized by cyclic voltammetry(CV) in 1 M KOH electrolyte using a three electrode system. Galvanostatic charge-discharge measurements made on the fabricated asymmetric supercapacitor gave a high specific capacitance of 17.33 F/g at a discharge current density of 0.2 A/g. Moreover, they showed an excellent cycle stability and better capacity retention of 92% after 2000 continuous charge-discharge cycles.

Keywords: Co_3O_4 Nanostructures, Co-Precipitation, Cyclic Voltammetry, Galvanostatic Charge-Discharge And Asymmetric Supercapacitor.

I. INTRODUCTION

Increasing demand in the need of global-energy drives the development of alternative or non conventional energy sources with high power and energy densities [1]. Batteries, fuel cells, and supercapacitors are typical non-conventional energy devices which are based on the principle of chemical-to-electrical energy conversion. They find wide spread applications in consumer electronics ranging from mobile phones, laptops ,digital cameras, emergency doors and hybrid vehicles etc. [2].

Supercapacitors are one of the newest innovations in the field of electrical energy storage, and will find their place in many applications where energy storage can help to smoothing of strong and short time power. It provides a bridge between batteries and the dielectric capacitor, and also provides better power and energy densities, high durability, flexible operating temperature, long cycle life, environmental friendliness and safety [3–5]. Based on different energy storage mechanisms, supercapacitors could be classified into two categories: double-layer capacitors (EDLCs) and electrochemical pseudocapacitors (EPCs). The capacitance of EDLCs is based on charge separation at the electrode/electrolyte interface, while the capacitance of EPCs arises from fast and reversible faradic redox reactions that can occur within the electroactive materials.Pseudocapacitors have higher energy density with the best properties exhibited by hydrated RuO_2 [6], but relatively high cost, poor rate capability and environmentally poisonous nature, induced the exploration of lower cost transition metal oxides such as MnO_2, Co_3O_4, NiO, Fe_2O_3. Among the transition metal oxides, Co_3O_4 is found to be one of the best alternate material due to its non-toxic, natural abundance, good redox property, and high theoretical specific capacitance [7,8].

Cobalt oxide has been synthesized using a variety of methods such as sol–gel [9], reflux [10] and hydrothermal [11] and Microwave assisted synthesis.[12] We report a facile synthesis and characterization of Co_3O_4 nanostructures on its utilization as electrode material for supercapacitor applications by co-precipitation method.

II. METHODS AND MATERIAL

A. Materials Used

All the chemicals are of extra pure and used without any further purification. Cobalt(II)chloride hexahydrate($CoCl_2 .6H_2 O$),sodium hydroxide are obtained from Merck, Activated carbon, Black Pearl Carbon -15nm,1475m^2g^{-1} (Cabot Corporation), Polyvinylideneflouride(PVdF)(Aldrich), N-methyl-2-pyrrolidone(NMP)(Merck).Distilled water is used throughout the process.

B.Synthesis of Co_3O_4 nanoparticles

The co-precipitation process is performed as follows: a solution containing 0.02M of $CoCl_2 .6H_2 O$ is added drop wise to a solution of sodium hydroxide having a concentration of 0.5M and pH 9 with continuous stirring for 2 hours at 90^o C. The precipitate is formed immediately and remained in the mother solution which is placed in a water bath for 4 hours. After cooling, the precipitate is filtered and washed repeatedly with distilled water until traces of sodium chloride formed during the reaction is removed. The precipitate is dried in a hot air oven for 2 hours and then it is ground well and is calcined at 350^oC for 4 hours to get cobalt oxide nanoparticles.

C. Material Characterization:

The powder X-ray diffractometer (Ultimate Rukagu IV) is recorded from 5 to 80^o using Cu-kα radiation (λ = 0.15408nm) at room temperature. The step size and scan rate are set at 0.1 ^{o} and 2^o min^{-1} respectively. FTIR spectra is recorded by FTIR spectrometer(SHIMADZU) in the range 4000-400 cm^{-1} . The surface morphology is analysed by Scanning Electron Microscope (Hitachi,Model:S-3000N).

D. Electrochemical Characterization:

The electrochemical measurement is performed in a three electrode configuration comprising of the as-synthesized nanoparticles based electrode, a platinum electrode and Ag/AgCl that serve as the working, counter and reference electrodes, respectively and 1M KOH as electrolyte using an electro- chemical analyzer (VSP, Bio-Logic, France). Cyclic voltammogram (CV) is carried out at different scan rates (5,10, 25, 50 and 100 mVs- 1) in the potential window of 0 to + 0.5V. The working electrode is prepared by mixing the as-synthesized nanoparticles, black pearl carbon, and polyvinylidene difluoride (PVdF) in N-methyl pyrrolidine (NMP) as binder at the ratio of 90:5:5 wt% to form slurry. This slurry is pasted on 1 cm^2 stainless steel sheet and vacuum dried at 80 ^oC for 2 hours.

D. Electrode Preparation: Coin type cell assembly

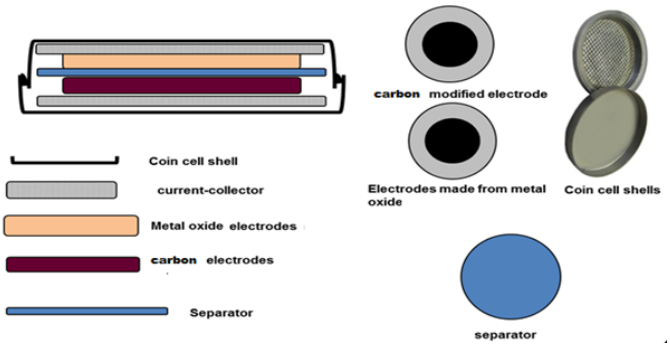

Figure 1. Coin Type Cell Assembly

The electrochemical performance of the prepared powder of synthesized nanoparticles are investigated using two-electrode coin-type cells (CR 2032) with steel foil as reference electrode**.(Fig.1)** The working electrode is prepared by mixing the as-synthesized nanoparticles , black pearl carbon, and polyvinylidene difluoride (PVdF) in N-methyl pyrrolidine (NMP) as binder at the ratio of 90:5:5 wt% to form slurry. The working electrode is assembled by coating the slurry of the synthesized nanoparticles on an aluminium foil current-collector of 1 cm in diameter and dried in an oven at 80 ^oC for 2 hours. The weight of the active material is determined by weighing the Al foil before and after pressing the powders. The supercapacitive behaviour is investigated in alkaline (1 M KOH) electrolyte. In the asymmetry assembly, the working electrode fabricated using the synthesized Co_3O_4 nanoparticles is used as the positive electrode while activated carbon is used as the negative electrode. The electrodes are soaked in the electrolyte for about 10 mins before assembled in the coin cells. A polypropylene (PP) film (Cellgard 2400) is used as the separator.

III. RESULTS AND DISCUSSION

A. X-ray Diffraction Analysis(XRD)

Fig 2 shows the XRD pattern of Co_3O_4 nanoparticles after calcination. The peak positions appearing at 2θ ≈18.9° ,31.2° ,36.8°,38.5°, 44.5° ,59.3° , 65.2° can be readily indexed as (111), (220) ,(311),(222), (400),(511), (440) crystal planes of Co_3O_4 respectively.

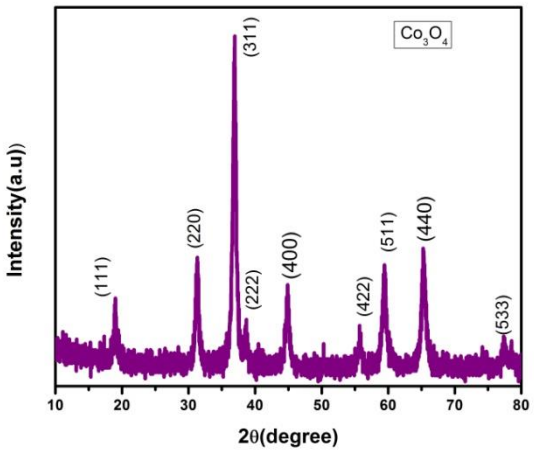

Figure 2. XRD patterns of Co_3O_4 nanoparticles calcined at 350° C

All reflections can be indexed to cubic spinel phase of Co_3O_4 and Fd3m space group with a lattice constant of 8.084A° [13-15] which agrees well with the standard data (JCPDS no 043–1003). The average crystallite size is calculated using Debye-Scherer equation (1), [16]

$$D = \frac{k\lambda}{\beta \cos\theta} \quad \text{-------- (1)}$$

where D(nm) is the crystallite size, k(0.9), λ(0.154nm) is the K_α component wavelength of Cu radiation source, β is the full width at half maximum of individual observed peak and θ is the Bragg's angle. The average crystallite size of about 14.61 nm is calculated using Debye-Scherer equation. It is observed that the peak intensity increases with a narrowing down of particle size with high purity on calcination [17].The broad peaks indicate that the overall morphology of the as-prepared Co_3O_4 is nanocrystalline [18].

B. FTIR spectral studies

The FTIR spectra of Co_3O_4 in Fig. 3 shows two strong absorption peaks at 659 cm^{-1} and 568 cm^{-1} . The absorption band at 568 cm^{-1} is assigned to Co-O stretching vibration mode [19] and 659 cm^{-1} is assigned to the bridging vibration of O-Co-O bond[20].

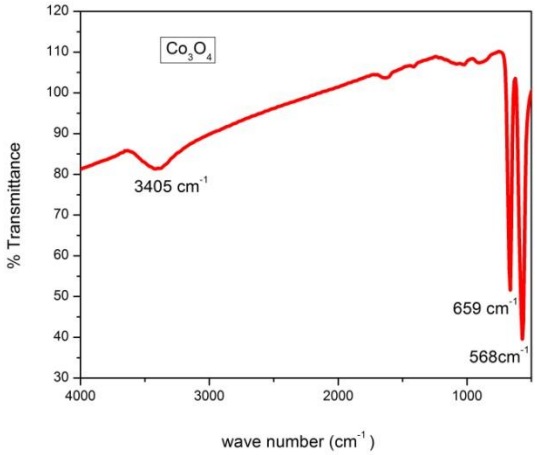

Figure 2. FTIR spectrum of Co_3O_4 nanoparticles

The peak at 3417 cm^{-1} relates to stretching vibration of the interlayer water molecule [21]. The FTIR spectra confirm the successful formation of pure Co_3O_4 nanoparticles.

C. SEM Analysis

The FE-SEM image of Fig 4 shows that the Co_3O_4 nanoparticles are spherical, homogenous and agglomerated with average size of 11nm.

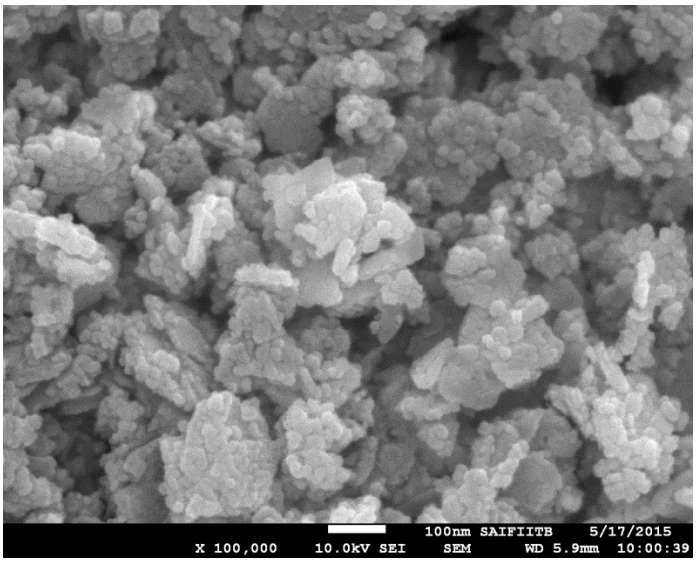

Figure 4. Surface Morphology of Co_3O_4 nanoparticles

The calcination process has left behind pores which allows facile penetration of electrolyte during electrochemical reaction. The nanocrystallites tend to agglomerate during synthesis or delivery process due to

their high surface area and surface energy. For Co_3O_4 nanoparticles, the agglomeration are purely due to the magnetic induction between the particles.[22]

D. CV Studies

To explore the potential application of the as synthesized sample, the electrochemical performance of the active material is investigated using a three-electrode system with Co_3O_4 as the working electrode at different scan rates ranging from 5 to 100 mV s−1 within the potential window 0 to 0.5 V as shown in Fig.5. The shape of the CV curve is different to that of the electric double layer capacitance, indicating that the two strong peaks are based on a redox mechanism. The redox peaks consisting of an anodic peak at 0.42 V and a cathodic peak at 0.32 V , corresponds to the reversible reactions of Co^{3+}/ Co^{4+} associated with anions OH^-.

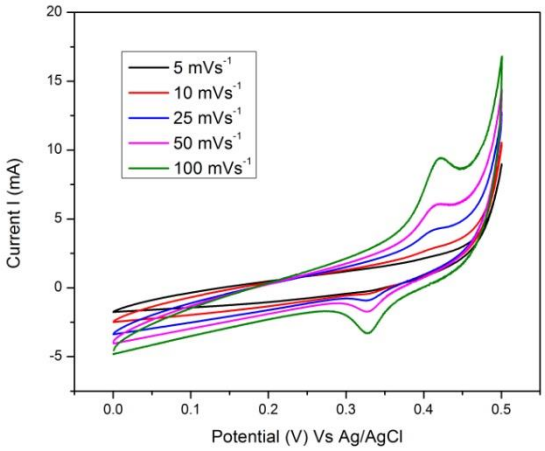

Figure 2. CV curves of Co_3O_4 based electrode in 1 M KOH at various scan rates

In the CV curve, the anodic and cathodic peaks are not symmetric due to kinetic irreversibility in the redox process [23]. With the increase of scan rate, the current response increases accordingly, while no significant change in the shape of CV curves is observed, indicating the good rate property of the electrode material. The pseudocapacitive behavior of Co_3O_4 in alkaline electrolyte are based on following equations [24,25].

$$3[Co(OH)_3]^- \leftrightarrow Co_3O_4 + 4H_2O + OH^- + 2e^- \quad (2)$$

$$Co_3O_4 + H_2O + OH^- \leftrightarrow 3CoOOH + e^- \quad (3)$$

$$CoOOH + OH^- \leftrightarrow CoO_2 + H_2O + e^- \quad (4)$$

The specific capacitance (Cs,) values at different scan rates in the CV measurement are calculated using equation (5) [26];

$$Cs = \frac{S}{2\Delta V v m} \left(\frac{F}{g}\right) \quad -(5)$$

where S is the area under the curve of CV loop(mA-V) , ΔV is the applied potential window(V), v is the scan rate (mVs^{-1}) and m (g) is the mass of the active electrode material. It is common practice to use 0.5 to 1 mg of the active material as the electrode [27,28]. The specific capacitance calculated using equation (5) at different scan rates of 5, 10, 25, 50 and 100 mV s^{-1} are found to be 552, 340, 176, 104.72, and 63.58 F g^{-1}, respectively. The Co_3O_4 nanostructure's morphology provides a large electroactive surface area and fast solid state diffusion of OH^- ions for highly feasible redox reaction and thus, the Co_3O_4 nanoparticles shows higher specific capacitance of 552 F g^{-1} .

E. Galvanostatic Charge-Discharge Cycling (GCD)

The real device which exhibits the practical application of supercapacitor is two electrode system rather than three electrode configuration. The important aspect of our work is the fabrication of asymmetric supercapacitor device(ASC) with the working electrode (Co_3O_4) used as the positive electrode and commercially available activated carbon used as the negative electrode. To fabricate asymmetric supercapacitor device, it is important to find the mass balance between the positive and negative electrode. The mass balance between the positive and negative electrodes is calculated to be

$$\frac{m^+}{m^-} = \frac{C^-}{C^+}\frac{V^-}{V^+} \quad ---- (6)$$

where C+ & C− are the specific capacitances, V+ & V− are the optimum voltage windows and m+ & m− are the active masses for positive and negative electrodes respectively. Using the specific capacitances of activated carbon reported by Shen Wang et.al., (C− = 135 F/g) and the calculated value of the specific capacitances of Co_3O_4 (from CV curve) (C+ = 552 F/g) ,V+ & V− are 0.5V , the required mass ratio for positive and negative electrode material ($m+/m-$) is estimated as 0.2 at 5 mV s−1. ASC is fabricated with m+ = 1mg and m− = 5 mg.

Galvanostatic charge-discharge is the most reliable and accurate method for evaluating the supercapacitance of electrodes. Hence GCD measurements are applied at a current density of 0.2 A/g to evaluate the electrochemical properties and calculate the specific capacitance of the asymmetric supercapacitors. The GCD curve of Fig. 6 shows that the charge and discharge curves are not perfectively symmetry which may be attributed to internal resistance and over potential and also due to the pseudocapacitance behavior of the positive electrode resulting from electrochemical adsorption or redox reactions at the interfaces between the electrodes and the electrolyte.

The specific capacitance is calculated from GCD curves using equation (7) [29-31]

$$C_s = 4 \text{ X } \frac{I \, X \, T_d}{V \, X \, M} \qquad \text{--- (7)}$$

where C_s is the specific capacitance (F/g), I is the constant discharge current, T_d is the discharge time, V is the discharging voltage after IR drop and M is the total mass of the positive and negative electrodes.

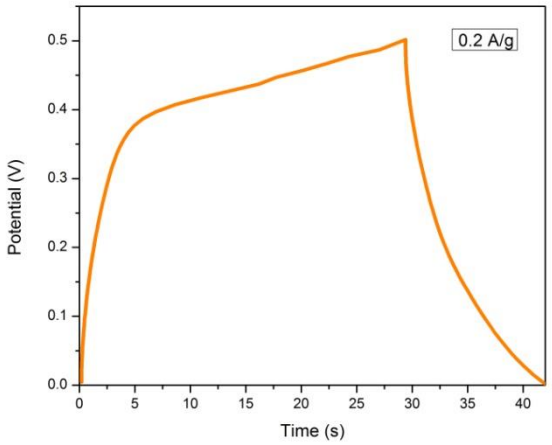

Figure 6. Galvanostatic charge-discharge curve of Co_3O_4 based electrode at 1 M KOH at a current density of 0.2 Ag^{-1}

The Specific Capacitance of the asymmetric supercapacitor calculated from discharge time according to the Equation(7) is 17.33F g^{-1} corresponding to the discharge current density of 0.2 A g^{-1}.Despite the high mass loading the specific capacitance is better than the reported specific capacitance of 11.76 F/g obtained for the MWCNT-Co3O4|MWCNT asymmetric supercapacitor assembly in 1 M Na_2SO_4 by Adekunle et.al [32]. In addition, the cycling performance of this asymmetric supercapacitor device is measured at a current density of 0.2 A/g from Fig.7 which shows Galvanostatic charge-discharge curves for few initial & final cycles of Co_3O_4 based asymmetric device. The asymmetric supercapacitor could keep ca. 92% of the initial capacitance after 2000 cycles. The capacitance retention is comparable or even better than few reported asymmetric devices such as NiO//C (50% after 1000 cycles)[33], Ni(OH)2–MnO2//RGO (76% after 3000 cycles)[34].

The reversibility of asymmetric device is further explored by measuring the Coulombic efficiency using equation (8) [35].

$$\eta = \frac{T_d}{T_c} \text{ x } 100 \qquad \text{----- (8)}$$

where T_d and T_c are discharge time after IR drop and charge time respectively.

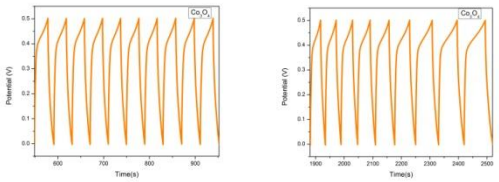

Figure 7. Galvanostatic charge-discharge curves for few initial & final cycles of Co_3O_4 based asymmetric device

From Fig.6, with T_d =13 s and T_c = 29.3 s the asymmetric device demonstrates excellent Coulombic efficiency of around 44% which shows its higher degree of reversibility. These superior capacitive performances, including good electrochemical reversibility, excellent rate capability, and high stability, indicate the suitability of our sample for the asymmetric supercapacitor application. Energy density(E) and maximum power density(P) of asymmetric device are calculated from GCD curves by using equations (9 and 10) respectively.

$$E \, (WhKg^{-1}) = \frac{1}{2 \, X \, 3.6} \text{ X } \frac{Cs}{4} \text{ X } V^2 \text{ ------(9)}$$

$$P_{max} \, (WKg^{-1}) = \frac{V^2}{4 \, X \, M \, X \, R} \text{ ----------(10)}$$

$$\text{Where R} = \frac{\Delta U}{2 \, X \, I}$$

where V(v) is the maximum voltage attained during charge, C_s is the specific capacitance (F/g), and M(Kg) is the total mass of the positive and negative electrodes and R(ohm) is the internal resistance determined from the voltage drop at the beginning of each discharge , ΔU (v) is the voltage drop during each discharge cycle which corresponds to IR drop, I(mA) is the constant discharge current. An energy density of 0.15 WhKg−1 at 595.23 WKg−1 approximately is calculated using Equations (9) and (10) respectively.

IV CONCLUSION

The present work demonstrated the facile synthesis of $Co_3O_4$with enhanced electrochemical performance.XRD studies confirmed the formation of the pure single phase cubic spinel structure. FTIR analysis showed two strong absorption peaks at 568 cm^{-1} and 659 cm^{-1} corresponding Co-O stretching vibration mode and to the bridging vibration of O-Co-O bond. The FE-SEM image showed that the Co_3O_4 nanoparticles were spherical, homogenous and agglomerated. Cyclic voltametric. studies carried out using a three electrode system showed the pseudo capacitance behaviour of the sample. Galvanostatic charge-discharge studies performed on the asymmetric supercapacitor revealed excellent cyclic performance, high specific capacitance and electrochemical stability of the as-synthesized sample thus demonstrating its high performance in supercapacitor applications.

IV. REFERENCES

[1]. B.E.Conway, Electrochemical supercapacitors, scientifc fundamentals and technological applications, Plenum, NewYork,1999.

[2]. A. Burke, J.Power Sources 91(2000)37–50.

[3]. B.E. Conway, Transition from Supercapacitor to Battery behavior in electrochemical energy storage, J. Electrochem. Soc. 138 (1991) 1539.

[4]. R. Kotz, M. Carlen, Principles and applications of electrochemical capacitors, Electrochim. Acta 45 (2000) 2483.

[5]. P. Simon, Y. Gogotsi, Materials for electrochemical capacitors, Nat. Mater. 7 (2008) 845.

[6]. Devadas, S. Baranton, T.W. Napporn, C. Coutanceau, Tailoring of RuO2 nanoparticles by microwave assisted Instant method for energy storage applications, J. Power Sources 196 (2011) 4044

[7]. T.Y. Wei, C.H. Chen, K.H. Chang, S.Y. Lu, C.C. Hu, Cobalt oxide aerogels of ideal supercapacitive properties prepared with an epoxide synthetic route, Chem. Mater. 21 (2009) 3228.

[8]. S.K. Mehar, G.R. Rao, Effect of microwave on the nanowire morphology, optical, magnetic, and pseudocapacitance behavior of Co3O4, J. Phys. Chem. C 115 (2011) 25543

[9]. G.A.Santos,C.M.B. Santos, S.W.DSilva, E.A Urquieta-Gonzalez, P.P.C Sartoratto, Sol–gel synthesis of silica–cobalt composites by employing Co3O4colloidal Dispersions, Colloids Surf. A: Physicochem. Eng. Aspects 395 (2012) 217.

[10]. S.K. Meher, G.R. Rao, Effect of microwave on the nanowire morphology, optical, magnetic, and pseudocapacitance behavior of Co3O4, J. Phys. Chem. C 115 (2011) 25543.

[11]. S.K. Meher, G.R. Rao, Ultralayered CO3O4 for high-performance supercapacitor applications, J. Phys. Chem. C 115 (2011) 15646

[12]. S.H. Jhung, T. Jin, Y.K. Hwang, J.S. Chang, Microwave effect in the fast synthesis of microporous materials: which stage between nucleation and crystal growth is accelerated by microwave irradiation? Chem. Eur. J. 13 (2007) 4410

[13]. Y.Y. Liang, S.J. Bao, H.L. Li, Nanocrystalline nickel cobalt hydroxides/ultrastable Y zeolite composite for electrochemical capacitors, J Solid State Electrochem. 11 (2007) 571.

[14]. Y. Li, K. Huang, S. Liu, Z. Yao, S. Zhuang, Meso-macroporous Co3O4 electrode prepared by polystyrene spheres and carbowax templates for supercapacitors, J. Solid State Electrochem. 15 (2011) 587.

[15]. M. Aghazadeh, Electrochemical preparation and properties of nanostructured Co3O4 as supercapacitor material, J. Appl. Electrochem. 42 (2012) 89.

[16]. B. Cullity, Elements of X-ray Diffraction, A.W.R.C. Inc., Massachusetts,1967.

[17]. R. Venkatnarayan, V. Kanniah, and A. Dhathathreya, Journal of Chemical Sciences, vol. 188, p. 179, 2006.

[18]. M.Q. Wu, J.H. Gao, S.R. Zhang, A. Chen, J. Porous Mater. 13 (2006) 407.

[19]. Estepa L and Daudon M, Biospectroscopy, 1997, 3, 347-369.

[20]. Wu S H and Chen D H, J Colloid Interface Sci., 2003, 259, 282-286.

[21]. Saravanan K, Govindarajan S, Chellappa D (2005) Preparation, Characterization, and Thermal Reactivity of Divalent Transition Metal Hydrazine Pyridine-2,n-dicarboxylates (n=3, 4, 5, and 6). Synth React. Inorg. Met.-Org. Chem. 34:353-370

[22]. Koutzarova T, Kolev S, Ghelev C, Paneva D and Nedkov I, Phys Stat Sol (c)., 2006, 3, 1302-1307

[23]. S.K. Meher, G.R. Rao, Effect of microwave on the nanowire morphology, optical, magnetic, and pseudocapacitance behavior of Co3O4, J. Phys. Chem. C 115 (2011) 25543.
[24]. L.Q. Mai, F. Yang, Y.L. Zhao, X. Xu, L. Xu, Y.Z. Luo, Nat. Commun. 2 (2011) 381e385.
[25]. M.Q. Wu, J.H. Gao, S.R. Zhang, C. Ai, J. Power Sources 159 (2006) 365e369.
[26]. Khalid, S. et al. Microwave Assisted Synthesis of Porous NiCo2O4 Microspheres: Application as High Performance Asymmetric and Symmetric Supercapacitors with Large Areal Capacitance. Sci. Rep. 6, 22699; doi: 10.1038/srep22699 (2016).
[27]. S. Devaraj, N. Munichandraiah, Effect of crystallographic structure of MnO2 on its electrochemical capacitance properties, J. Phys. Chem. C 112 (2008) 4406.
[28]. S.K. Meher, G.R. Rao, Ultralayered CO3O4 for high-performance supercapacitor applications, J. Phys. Chem. C 115 (2011) 15646.
[29]. Feng, J.-X., Ye, S.-H., Lu, X.-F., Tong, Y.-X. & Li, G.-R. Asymmetric Paper Supercapacitor Based on Amorphous Porous Mn3O4 Negative Electrode and Ni(OH)2 Positive Electrode: A Novel and High-Performance Flexible Electrochemical Energy Storage Device. ACS Appl. Mat. Interfaces 7, 11444-11451 (2015).
[30]. Luan, F. et al. High energy density asymmetric supercapacitors with a nickel oxide nanoflake cathode and a 3D reduced graphene oxide anode. Nanoscale 5, 7984-7990 (2013).
[31]. Chen, P.-C., Shen, G., Shi, Y., Chen, H. & Zhou, C. Preparation and Characterization of Flexible Asymmetric Supercapacitors Based on Transition-Metal-Oxide Nanowire/Single-Walled Carbon Nanotube Hybrid Thin-Film Electrodes. ACS Nano 4, 4403-4411 (2010).
[32]. Abolanle S. Adekunle, Bolade O. Agboola, Kenneth I. Ozoemena, Eno E. Ebenso, John A.O. Oyekunle, Oluwafemi S. Oluwatobi, Joel N. Lekitima, Int. J. Electrochem. Sci., 10 (2015) 3414 – 3430
[33]. Wang, D.-W., Li, F. & Cheng, H.-M. Hierarchical porous nickel oxide and carbon as electrode materials for asymmetric supercapacitor. J. Power Sources 185, 1563–1568 (2008).
[34]. Chen, H. et al. One-Step Fabrication of Ultrathin Porous Nickel Hydroxide-Manganese Dioxide Hybrid Nanosheets for Supercapacitor Electrodes with Excellent Capacitive Performance. Adv. Energy Mater. 3, 1636–1646 (2013).
[35]. Makgopa, K. et al. A high-rate aqueous symmetric pseudocapacitor based on highly graphitized onion-like carbon/birnessite-type manganese oxide nanohybrids. J. Mat. Chem. A 3, 3480-3490 (2015).